

## Performance analysis of a double-slope solar still with elevated basin — comprehensive study

Wissam H. Alawee<sup>a,\*</sup>, Suha A. Mohammed<sup>b</sup>, Hayder A. Dhahad<sup>b</sup>, F.A. Essa<sup>c</sup>,  
Z.M. Omara<sup>c</sup>, A.S. Abdullah<sup>d,e</sup>

<sup>a</sup>Control and Systems Engineering Department, University of Technology, Baghdad, Iraq, email: wissam.h.alawee@uotechnology.edu.iq

<sup>b</sup>Mechanical Engineering Department, University of Technology, Baghdad, Iraq, emails: 20050@uotechnology.edu.iq (S.A. Mohammed), hayder.a.dhahad@uotechnology.edu.iq (H.A. Dhahad)

<sup>c</sup>Mechanical Engineering Department, Faculty of Engineering, Kafrelsheikh University, Kafrelsheikh, Egypt, emails: fadlessa@eng.kfs.edu.eg (F.A. Essa), zm\_omara@yahoo.com (Z.M. Omara)

<sup>d</sup>Mechanical Engineering Department, College of Engineering, Prince Sattam bin Abdulaziz University, KSA, email: a.abdullah@psau.edu.sa

<sup>e</sup>Mechanical Power Engineering Department, Faculty of Engineering, Tanta University, Tanta, Egypt

Received 23 July 2020; Accepted 11 February 2021

### ABSTRACT

Solar distillation is an effective method of generating potable fresh water in areas where there is abundant sunshine with adequate water that is unfit for human consumption or other activities. In the current study, an experimental and theoretical analysis was performed to evaluate the productivity of a modified solar still having an elevated basin. This improvement was achieved by raising the basin inside the distiller. The elevated basin helps in reducing the thermal losses from the bottom and sides of the distiller because the air gap between the basin and both the bottom and sides of the distiller acts as an insulator. All tests were carried out under the weather conditions of the Baghdad-Iraq region during the months of February, March, April, and May. The average distilled water outputs per square meter for the experimental period were 3.03 and 4.37 L for the conventional solar still (CSS) and elevated-basin solar still (EBSS), respectively. The average percentage increment in the fresh water production from the EBSS was found to be 36.7% (relative to that of the CSS). It was evident that the theoretical model predicted the trends very well, with some deviations from the experimental values. The average difference between the theoretical and experimental findings in total productivity was found to be between 4% and 8%. The estimated average cost of the distillate water was \$0.027/L m<sup>2</sup> for the EBSS.

*Keywords:* Solar still; Desalination; Productivity; Double-basin still; Modified design

### 1. Introduction

Solar distillation has been introduced as a promising and sustainable method of producing drinkable fresh water. It is aided by a sustainable energy source and avoids the presence of any impurities. It is more likely used in remote areas, for example, small islands and other places with

sensible amounts of sunlight and on-going water. However, an inability to provide good numbers of solar distillers has prevented the increased use of their benefits worldwide.

A conventional double-slope solar distiller, as shown in Fig. 1, mainly suffers from a lack of productivity; the daily production generally varies from 2 to 3 L/m<sup>2</sup> of basin area [1]. This produced amount is considered to be

\* Corresponding author.

relatively low as compared with the productivity of modified solar stills, where researchers have used varying designs or improvements on the conventional design for the purposes of increasing productivity and performance. In a solar still, processes of evaporation and condensation occur alternately within the solar system with the aid of temperature differences between evaporation and condensation areas, producing fresh water. Variables that influence solar still efficiency are divided in two major categories. The first category comprises uncontrollable factors related to weather, climate, and geographical location, such as air temperature, wind speed and solar radiation. The second category comprises design factors, which can be controlled to achieve optimum performance.

In this study, we review the design factors employed by researchers in different ways to increase the output throughout the distillation by increasing the evaporation, increasing the condensation, or both. An initial heating process of the water in the distillation basin minimises the required period for evaporation, and thus speeds up the evaporation process (and productivity). The initial heating process can be conducted before the water enters the still by using a flat plate collector [2–4], solar concentrator [5], heat pipes [6] and mini solar ponds [7]. Other methods for increasing basin water temperature include the use of internal reflectors [8,9], external reflectors [10], or both [11,12]. These reflectors work by reflecting the sunlight on the absorption plate, helping provide extra heating for the distillation basin.

The evaporation rate in the distillation basin varies according to the area of surface absorption. With increased exposure to sunlight in the distillation basin, productivity increases. Many researchers have used various methods to enhance thermal performance between the water and the absorption plate, including the use of wavy or fin-shaped absorption plates [13,14], or by using specific distillation basin methods that help to improve the surface absorption area of cloths, wicks, and sponges [15,16]. The use of specific nanomaterials [17–20] in the distillation basin has been shown to contribute to increase the thermal performance between the absorption plate and water. Increasing the heat transfer increases the water temperature, leading to an increase of the difference in temperature between the condensation surface and water, and thus increased potable fresh water.

Some researchers have concentrated on improving the condensation area in the solar still as it is one of the key components that still affect the efficiency and productivity. The productivity of still systems is impacted by the temperature difference between the zones of evaporation and condensation. Cooling the glass covers in some way decreases the condensation surface temperature and improves thermal performance between the glass covers and the distillation basin water. Thus, it improves the productivity of the distilled water. To sustain a high difference in temperature, a number of researchers have used a method of cooling a glass cover by means of a flowing water film [21] or through airing by the use of an external fan [22,23]. Other researchers have used additional condensing coils attached to the solar still, which contribute to increasing productivity; these are mainly applied in condensers in different shapes, or in internal designs [24] or

external designs [25,26]. Likewise, other researchers have examined the influence of changing the material of the top cover [27] or the inclination angle of the condensation area on the output of the solar stills [28,29].

Furthermore researchers have used additional different methods to achieve better performance and productivity, such as phase change materials [30], sun tracking systems [31], and humidification–dehumidification systems [32,33].

Over the last 10 years, many papers have been published regarding different designs for single-effect solar stills, for example, single- or double-sloped. Many of these designs enhanced the performance and efficiency of conventional solar stills (CSSs). These designs included fan solar stills [34], spherical and pyramid solar stills [35], wick solar stills [36], solar chimney and condensers [37], rotating wick solar stills [38], rotating discs solar stills [39], and solar stills with rotating drums [40].

In this context, the attempts are also made to increase the productivity of water by rising the basin of solar still. Based on the best knowledge of the authors, there is no study concerned about such modification. The elevated basin helps to reduce the losses from the bottom and sides of the distiller because the air gap between the basin and both of bottom and sides of the distiller acts as an insulator. So, the current study aims to analyse the performance of solar still with an elevated-basin (experimentally and theoretically) under the weather of the city of Baghdad during a period of time from February to May 2019. In addition, the elevated-basin compared with CSS.

## 2. System design and experimentation

Two types of single-effect double-slope solar system were planned, installed and tested at the training and workshop center at the University of Technology, Baghdad, Iraq, to assess the performance and provide a comparison. The first was still a double-slope CSS, while the second solar was still modified from the CSS (that is, it was an elevated-basin solar still [EBSS]). Fig. 1 displays two solar stills, which are made in this analysis.

The solar systems were made of 1 mm galvanised steel. The basin water coated black paint to enhance radiation absorption. Glass covers with an inclination of 30° and thickness of 4 mm were used as a condensation surface. The side walls of the solar stills were insulated using glass wool. For feeding of salty water, a 40-L storage tank was used. The sizes of the distillation basin used in the CSS and EBSS were 125 cm × 60 cm × 1 cm, respectively. The dimensions and other additional details of the CSS and EBSS are given in Figs. 2 and 3, respectively.

In a CSS, the distillation basin rests on the base of the solar still. Therefore, the condensation area is limited and restricted by the dimensions of the solar still base, as shown in Fig. 2. Therefore, the double-slope CSS was modified to a double-slope EBSS. In the EBSS, the distillation basin was separated from the still base at a height of 30 cm from the base, as shown in Fig. 3. The elevated basin helps in reducing the thermal losses from the bottom and sides of the distiller because the air gap between the basin and both the bottom and sides of the distiller acts as an insulator.



Fig. 1. Photographs of tested solar stills: (a) CSS and (b) EBSS.

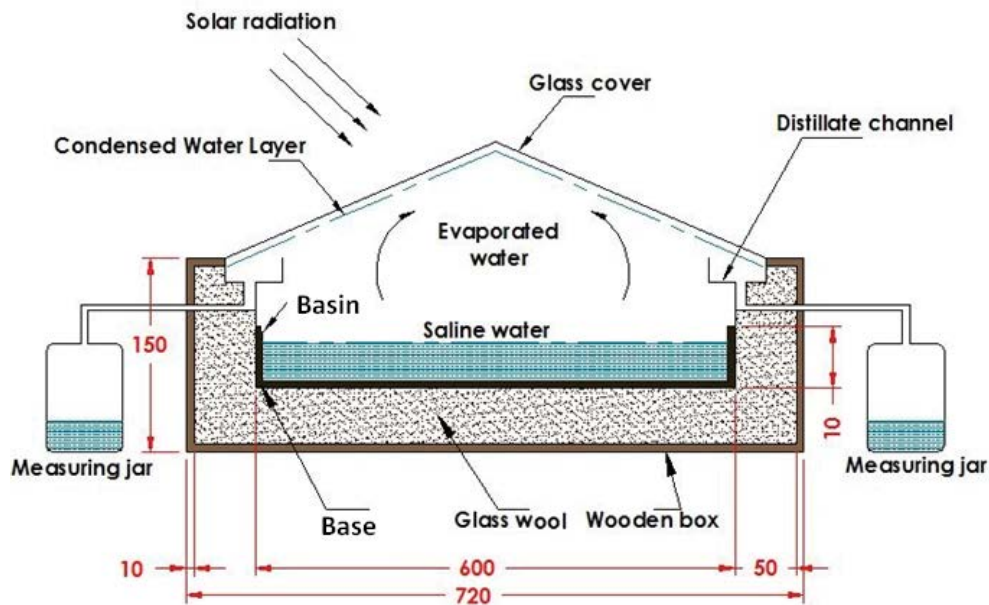


Fig. 2. Schematic of the CSS.

This modification increased the condensation surface area by 82.4% as compared with that of the CSS (Appendix A). In this work, the dimensions of the basin were fixed in both distillers. Indeed, the modified distillate has dimensions larger than conventional still, in order to generate an air gap between the base and the sides. This has the advantage of reducing the shading effect on the basin. To avoid the difference in the dimensions, productivity was calculated per square meter for the external dimensions of the two distillers.

Thermocouples (type T) have been used to measure the temperatures of the basin ( $T_b$ ), basin water ( $T_w$ ) and glass cover ( $T_g$ ). The accuracy of the thermocouple reading was within the range of  $\pm 0.2^\circ\text{C}$  to  $0.4^\circ\text{C}$ . The temperature of air was measured using a mercury thermometer. The ambient temperature was measured with a mercury thermometer. Solar intensity was measured by means of

a solarimeter ( $0\text{--}2,500\text{ W/m}^2$ ) with a precision of  $\pm 2\text{ W/m}^2$ . The volume of water collected was measured using a graduated 5-L-capacity container (with a precision of 3 mL). The experiments were conducted in Baghdad, Iraq ( $33^\circ 18' \text{ N}$ ,  $44^\circ 21' \text{ E}$ ) from 8:00 a.m. until 5:00 p.m. for 3-d chosen (between February and May, 2019). The salt water, glass cover, basin and air temperatures, solar intensity, and yield were recorded for every hour.

### 3. Experimental error analysis

The present work employed the proposed method of estimating the uncertainty of the results by Holman [41]. Assume that a set of measurements were carried out to determine  $n$  number of experimental parameters. Let  $R$  be the desired experimental result obtained based on these measurements.

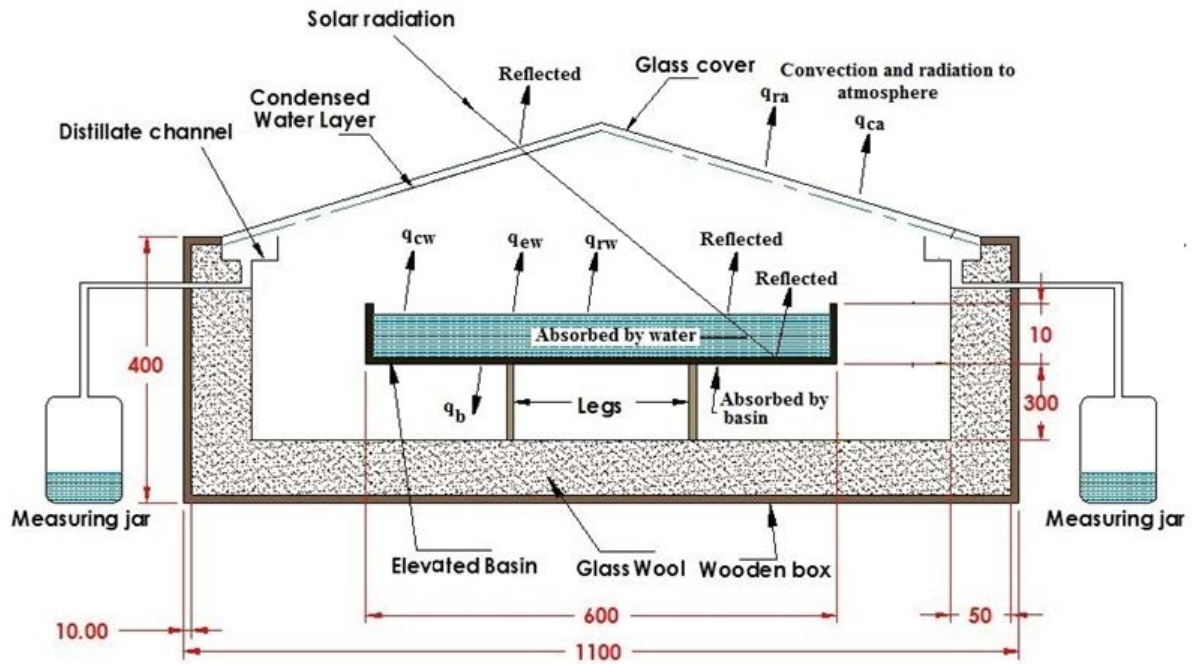


Fig. 3. Schematic of the EBSS.

Thus;

$$R = R(X_1, X_2, X_3, \dots, X_n) \tag{1}$$

Let the uncertainty in the result is  $W_R$  and  $W_1, W_2, W_3, \dots, W_n$  are the uncertainties in the independent variables. Hence,  $W_R$  can be computed using the proposed equation by Holman [41] as follows:

$$W_R = \left[ \left( \frac{\partial R}{\partial X_1} W_1 \right)^2 + \left( \frac{\partial R}{\partial X_2} W_2 \right)^2 + \dots + \left( \frac{\partial R}{\partial X_n} W_n \right)^2 \right]^{1/2} \tag{2}$$

If the result and measured parameters have a known relationship and the uncertainty associated to each measurement is also known, then  $W_R$  can be evaluated using Eq. (2). The uncertainties of the experimental measuring devices are presented in Table 1. The ratio between the least count of the device and the minimum output value gives the minimum error [42].

The hourly distillate,  $m = f(h)$ , where  $h$  = the height of water in the flask. From Eq. (2), the total uncertainty associated with the hourly production of the freshwater condensate can be reduced to:

$$W_m = \left[ \left( \frac{\partial m}{\partial h_1} W_{h_1} \right)^2 \right]^{1/2} \tag{3}$$

The calculation of thermal efficiency ( $\eta$ ) is also associated with uncertainties. The equation of  $\eta$  is  $\eta_{th} = \frac{\dot{m} \times h_{fg}}{A \times I(t)}$ .

Since  $A$  is constant and assuming  $h_{fg}$  is constant then,

Table 1  
Experimental uncertainty errors and measurement precision

Instrument	Accuracy	Range	Error, %
Solarimeter	$\pm 1 \text{ W/m}^2$	0–5,000 $\text{W/m}^2$	1.5
Wind anemometer	$\pm 0.1 \text{ m/s}$	0.4–30 $\text{m/s}$	3
Thermocouples	$\pm 0.1^\circ\text{C}$	0°C–100°C	1.3
Measuring jar	$\pm 5 \text{ mL}$	0–2,000 $\text{mL}$	2

$$\eta_{th} = f(\dot{m}, I(t)) \tag{4}$$

From Eq. (2), the total uncertainty of  $\eta$  can be derived as follows:

$$W_{\eta_{th}} = \left[ \left( \frac{\partial \eta_{th}}{\partial \dot{m}} W_{\dot{m}} \right)^2 + \left( \frac{\partial \eta_{th}}{\partial I(t)} W_{I(t)} \right)^2 \right]^{1/2} \tag{5}$$

Accordingly, the subsequent errors associated with the calculated quantity of daily productivity are about  $\pm 1.25\%$ . Accordingly, the resulting errors associated with the calculated  $\eta$  of the solar still are about  $\pm 2.7\%$ .

#### 4. Mathematical model

Fig. 3 displays the schemas for the various heat transfer modes in the double slope solar still. Such types are convection, heat and evaporation. The CSS and EBSS mathematical models are based on the energy balances of the glass, basin water and basin. The following premises are considered in the determination of equations for the energy balance.

- There is no leakage from the two solar stills.
- The heat that the glass surface absorbs is equal to the heat that the vapour rejects; therefore, all vapours are converted into distilled water.
- The temperature gradients along the depth of the water and the glass cover thickness are negligible.

The energy balance is explained as follows based on the above.

#### 4.1. Glass cover

The energy obtained from the glass cover includes the energy absorbed from the sun ( $I_T \alpha_g$ ) and the energy transfer from the basin water across evaporation ( $q_{e,wg}$ ), convection ( $q_{c,wg}$ ), and radiation ( $q_{r,wg}$ ). This obtained energy would partially raise the temperature of the glass ( $M_g C_{p,g} / dt$ ), and partially pass it by convection ( $q_{c,ga}$ ) and radiation ( $q_{r,ga}$ ). The glass cover's energy balance can be the following [43]:

$$(\alpha_g I_T) A_g + q_{e,wg} + q_{c,wg} + q_{r,wg} = M_g C_{p,g} \frac{dT_w}{dt} + q_{c,ga} + q_{r,ga} \quad (6)$$

Evaporative, convective and radiative energy between water and glass is given as follows [43]:

$$q_{e,wg} = h_{e,wg} (T_w - T_g) \quad (7)$$

$$q_{c,wg} = h_{c,wg} (T_w - T_g) \quad (8)$$

$$q_{r,wg} = h_{r,wg} (T_w - T_g) \quad (9)$$

In the above,  $h_{e,wg}$  represents the coefficient of heat transfer of evaporation between the still water and glass ( $W/m^2$ ), and is estimated as follows [44]:

$$h_{e,wg} = 16.276 \times 10^{-3} h_{e,wg} \left( \frac{p_w - p_g}{T_w - T_g} \right) \quad (10)$$

Here,  $p_w$  is the partial water vapor pressure at the  $T_w$  and  $p_g$  is partial water vapor pressure at the  $T_g$  (in Pa).

In addition,  $h_{c,wg}$  is the coefficient of convective heat transfer between the basin water and glass ( $W/m^2$ ), and is defined as follows [44,45]:

$$h_{c,wg} = 0.884 \left[ (T_w - T_g) + \frac{(p_w - p_g)(T_w + 273)}{(268.9 \times 10^3 - p_w)} \right]^{1/3} \quad (11)$$

$h_{r,wg}$  represents the coefficient of radiation heat transfer between the glass cover and basin water ( $W/m^2$ ), and is defined as follows [45]:

$$h_{r,wg} = \epsilon_{eq} \sigma \left[ (T_w + 273)^2 + (T_g + 273)^2 \right] \left[ T_w + T_g + 546 \right] \quad (12)$$

The transfer of energy by convection and radiation between glass and air is given as [45]:

$$q_{c,ga} = h_{c,g-a} (T_g - T_a) \quad (13)$$

$$q_{r,ga} = \epsilon_g \sigma \left[ (T_g - 273)^4 - (T_{sky} - 273)^4 \right] \quad (14)$$

where

$$h_{c,ga} = 2.8 + 3V \quad (15)$$

$$h_{r,ga} = \epsilon_g \sigma \left[ \frac{(T_g - 273)^4 - (T_{sky} - 273)^4}{(T_g - T_a)} \right] \quad (16)$$

#### 4.2. Water basin

The energy absorbed in the basin water is transferred partly into the basin ( $q_{c,bw}$ ), and mirrored in part to the glass cover by evaporation ( $q_{e,wg}$ ), convection ( $q_{c,wg}$ ), and radiation ( $q_{r,wg}$ ). The residual energy would increase the temperature of the basin water by  $M_w dT/dt$ . The water basin's energy balance is shown as follows [43]:

$$(\alpha_w I_T) A_w + q_{c,bw} = M_w C_{p,w} \frac{dT_w}{dt} + q_{e,wg} + q_{c,wg} + q_{r,wg} \quad (17)$$

The heat transfer by convection between the basin and water is given as follows [43,45]:

$$q_{c,bw} = h_{c,bw} (T_b - T_w) \quad (18)$$

The coefficient of convective heat transfer between the basin and water ( $h_{c,bw}$ ) is  $135 W/m^2 K$  [43].

#### 4.3. Basin

The solar intensity ( $\alpha_b I_T$ ) increases the energy of the basin absorber layer. This extracted energy is equal to the amount of the energy produced from the basin and the energy lost by the air and water convection. The equation of energy balance for the basin is as follows [43]:

$$(\alpha_b I_T) A_b = M_b C_{c,b} \frac{dT_b}{dt} + q_{c,bw} + q_{loss} \quad (19)$$

The heat losses from the basin to ambient air [46] are as follows:

$$q_{loss} = U_o (A_b + A_s) (T_b - T_a) \quad (20)$$

where  $U_o = 1/R_t$

$$R_t = R_1 + R_2 + R_3$$

$$R_1 = L_{air\ gap} / K_{air\ gap}$$

$$R_2 = L_{glass\ wool} / K_{glass\ wool}$$

$$R_3 = L_{wooden\ box} / K_{wooden\ box}$$

where  $K$  and  $L$  are thermal conductivity and the thickness of the insulation; respectively.

The thickness of the insulation in the conventional still is smaller than that of the modified still due to the still geometry, then for the modified still the heat loss coefficient from basin and sides is smaller than that for conventional still.

4.4. Condensate flow rate calculation

The amount of water condensed (productivity) can be estimated as follows [47]:

$$m_w = \frac{q_{e,w-g}}{h_{fg}} = \frac{h_{e,w-g}(T_w - T_g)}{h_{fg}} \tag{21}$$

In the above,  $h_{fg}$  is latent heat of vaporisation, and the values are calculated as follows [47]:

$$h_{fg} = \left( 597.49 - 5.6625 \times 10^{-1} T_w + 1.5082 \times 10^{-4} T_w^2 - 3.2764 \times 10^{-6} T_w^3 \right) \times 4.1868 \tag{22}$$

Initially, the time period was supposed as 5 s, and the temperatures of the glass, water, and basin were considered as the ambient temperature. The engineering equation solver program was used to solve Eqs. (1), (12) and (14) to predict variations in glass ( $dT_g$ ), saline water ( $dT_w$ ) and basin temperature ( $dT_b$ ). Experimentally determined solar intensity values and ambient temperatures were used for the respective hour and day. The parameter was redefined for the next step. Table 2 gives the physical input parameters used for the mathematical modelling.

5. Results and discussions

Figs. 4 and 5 display the effects of the mean time-to-moment fluctuations in weather conditions (solar

radiation and air temperature) between February and May. In these figures, the test days were divided into four categories, according to the monthly radiation level. The first is for days with average radiation of approximately 271 W/m<sup>2</sup> (February), the second for 382 W/m<sup>2</sup> (March), the third for 504 W/m<sup>2</sup> (April), and the fourth for 650 W/m<sup>2</sup> (May).

The solar intensity tends to increase in the morning, reaches the highest value in the noon and then begins to decrease after 1:00 p.m. The solar intensity during May is higher than in other months, and the maximum recorded value is 860 W/m<sup>2</sup>. Fig. 5 shows the change in ambient temperature on an hourly basis. The ambient temperature is found to be lower in the morning, and then increases with rising solar radiation.

The temperatures describing the behaviour of the solar stills are graphically presented in Figs. 6a–d and 7a–d for an average of three test days in each month. These figures illustrate the empirical and mathematical hourly changes of the water basin, glass and basin temperatures in the CSS and EBSS. The trends of temperatures for all solar stills are found to be similar. The basin temperatures are found to be the highest, followed by basin water and glass temperatures. The temperature rises through the daytime,

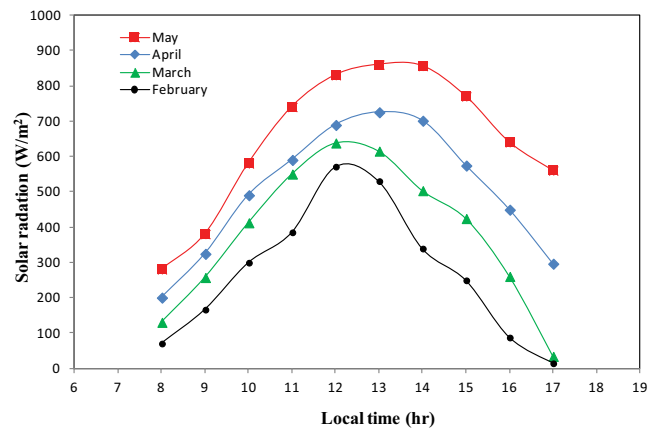


Fig. 4. Variation mean solar intensity with time during February–May.

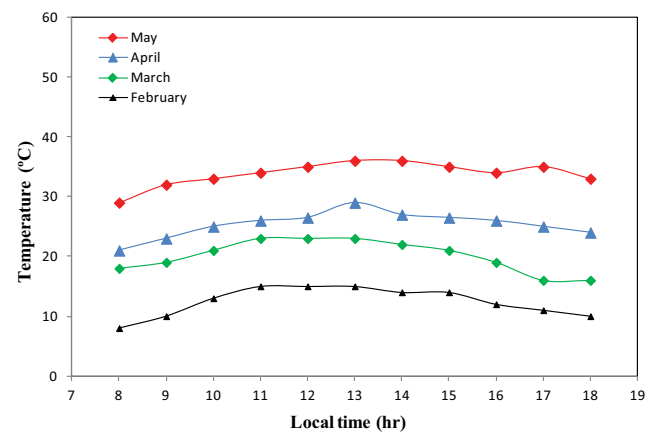


Fig. 5. Ambient temperature variation during February–May.

Table 2  
Physical input parameters used for mathematical modelling

Parameters	Value
Mass of glass, $M_g$	10.0 kg for CSS 18.5 kg for EBSS
Specific heat of glass, $C_{p,g}$	800 J/kg K
Area of glass, $A_g$	0.86 m <sup>2</sup> for CSS 1.58 m <sup>2</sup> for EBSS
Absorptivity of glass, $\alpha_g$	0.0475
Emissivities of water, $\epsilon_w$	0.96
Emissivities of glass, $\epsilon_g$	0.88
Mass of water, $M_w$	15 kg
Specific heat of water, $C_{p,w}$	4,187 J/kg °C
Absorptivity of water, $\alpha_w$	0.05
Area of water, $A_w$	0.75 m <sup>2</sup>
Mass of basin, $M_b$	5.2 kg
Specific heat of basin, $C_{p,b}$	473 J/kg °C
Absorptivity of basin, $\alpha_b$	0.95
Area of the basin plate, $A_b$	0.75 m <sup>2</sup>

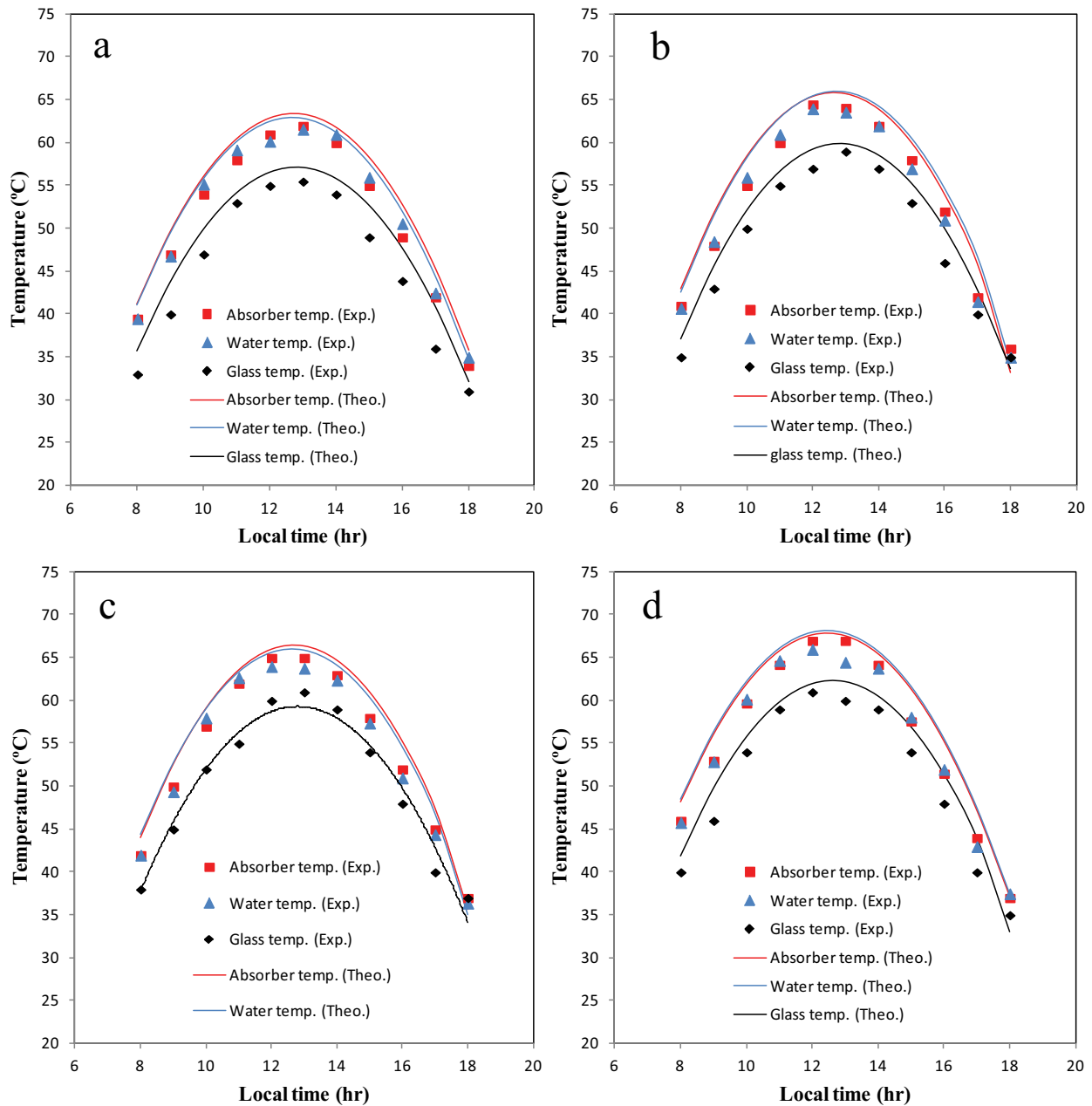


Fig. 6. Experimental and theoretical variation of different hourly temperatures for conventional solar still for February, March, April and May.

reaching the maximum from 12:00 p.m. to 1:00 p.m. These results are found to be similar to that obtained by other researchers [10,49–51]. The lowest measured temperature in the water basin is found in the CSS, whereas higher temperatures are found when the EBSS is used. The raise in the water temperature can be attributed to the improvement of the thermal performance of the EBSS. The maximum water temperature in the month of May is reached for two stills as the solar intensity is higher. The highest distillation basin water temperature is found to be 67.5°C and 75.6°C for the CSS and EBSS, respectively, during May, as illustrated in the figures. The increase in the water temperature of the EBSS can be attributed to the EBSS decreasing the loss from the

walls bottom and sides owing to the spaces left between the water basin and the walls. This confirms that the modified design overcomes the shortcomings of the CSS.

Figs. 6 and 7 also depict a comparison of measured temperatures with predicted temperatures from a mathematical model. It can be found that both the experimental and mathematical findings show the same trend in temperature rises and decreases with respect to time. The average difference for water, glass, and basin temperatures between the mathematical and experimental results is 4.1%, 4.5% and 6.0%, respectively.

The hourly yields of the two solar stills (for all of the test months) are presented in Figs. 8 and 9. In each of these

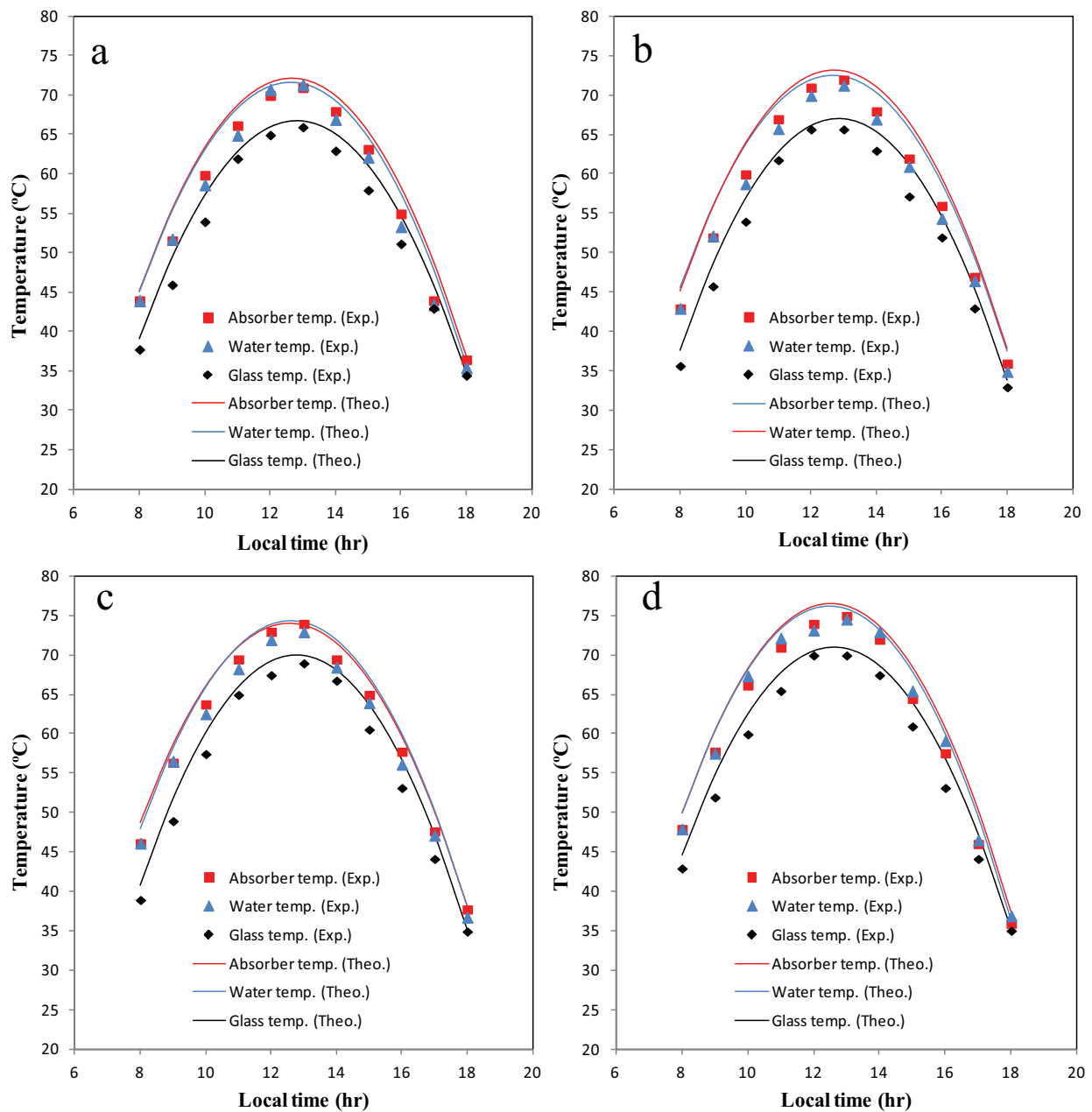


Fig. 7. Experimental and theoretical variation of different hourly temperatures for elevated basin solar still for February, March, April and May.

figures, the productivity is observed to increase between 8:00 a.m. and 1:00 p.m. as the solar intensity arrives its most extreme worth during the day, after which the productivity decreases as the solar intensity reduces, until the experiment is stopped at 5:00 p.m. The distillate water output during the month of May is higher than that of the other months (February, March, and April). The maximum hourly productivity per unit area is found from 12:00 p.m. to 1:00 p.m. at 0.493 and 0.621 L for the CSS and the EBSS, respectively.

On May, the average CSS and EBSS distillate water yields per square meter were 0.363 and 0.47 mL, respectively. Therefore, the hourly productivity increased in the EBSS. This is because the difference in temperature

between saline water and glass in EBSS is higher than CSS at this period. In addition, the EBSS condensation region is greater than that of the CSS. Hence, the condensation rate was increased, and the vaporisation rate was increased. The EBSS also reduced the loss of heat from the walls and the bottom due to the air gap between the basin water and the walls. This confirms that the modified design overcomes the shortcomings of the CSS. The mean difference between the mathematical and experimental results is found to be 6%–8% for the total productivity.

The accumulated productivity values from the CSS and EBSS as a function of the time from 8:00 a.m. until 5:00 p.m. are shown in Fig. 10. As appeared in the figure, the

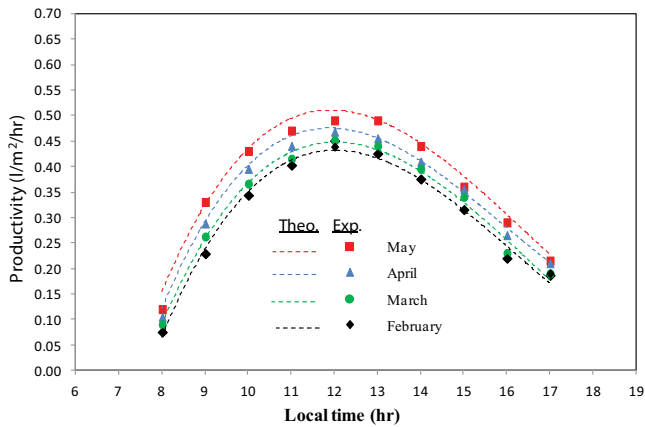


Fig. 8. Hourly variation productivity for the CSS.

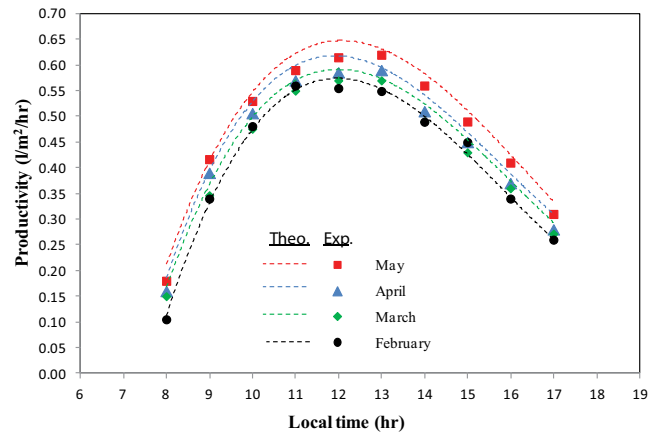


Fig. 9. Hourly variation productivity for the EBSS.

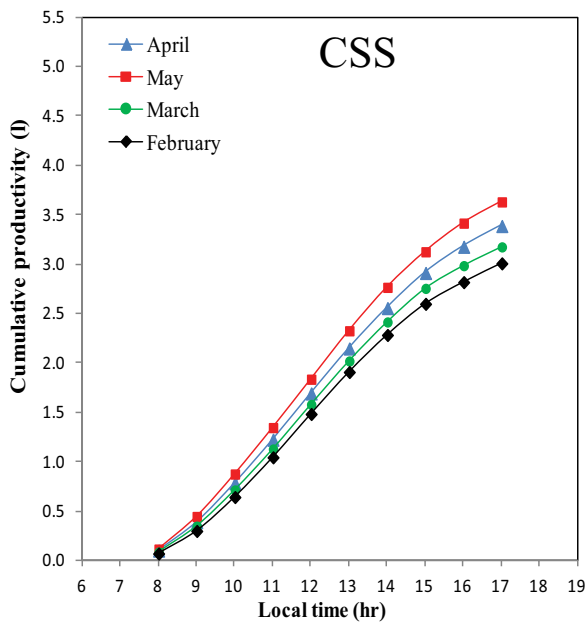


Fig. 10. Variation of cumulative productivity from CSS and EBSS.

maximum daily productivity values are found in the long stretch of February for both solar stills. The daily amount of productivity of the CSS is 3.02, 3.17, 3.39 and 3.63 L /m<sup>2</sup> of February, March, April and May months, respectively. The productivity values of the EBSS are 4.14, 4.22, 4.42 and 4.73 L/m<sup>2</sup> of February, March, April and May months, respectively. The performance improvement of the EBSS is estimated to be between 37% and 47.0%. In addition, the yield in the months of February, March, April and May was about 4.1–4.7 L/d for several average days (three clear days).

The variation of the productivity as a function of solar intensity for the CSS and EBSS is illustrated in Fig. 11. It is clearly evident that the productivity of the EBSS is superior to that of the CSS. Fig. 12 shows the varieties of the profitability of two solar stills as a function of mean solar radiation. It is apparent that both solar stills have average productivity values that increase linearly compared with average solar intensity. With an average solar intensity of

650 W/m<sup>2</sup>, the optimum yield of 0.472 L/m<sup>2</sup> is reachable. The rise in fresh water production from EBSS is 32.4% relative to the CSS.

## 6. Economic analysis

An economic analysis offers the correct distillate water cost value associated with the capital expenditure, and the desalination system operating and maintenance costs. The economic analysis is based on a method defined in the literature [52,53] to estimate the distilled water unit cost in US\$/L. Solar stills are characterized by low annual operating costs and high initial costs. The capital costs (*P*) of the CSS and EBSS are, respectively, \$125.7 and \$150 according to the Iraqi market, as shown in Table 3. Appendix B sets out the equations used for the economic analysis.

The overall fixed CSS cost is almost \$125.7 and the overall fixed EBSS cost is almost \$150. Experimental research

Table 3  
Fabricated cost of solar stills

Components	Cost in \$	
	Conventional solar still	Elevated basin still
Galvanized iron	15.0	25.0
Water tank	20.6	20.6
Wooden box	19.3	22.2
Pipe network	12.4	12.4
Iron stand	13.6	16.0
Paint	8.0	8.0
Glass cover	16.2	19.0
Silicon rubber	5.0	5.0
Fabrication	15.6	21.8
Total capital cost ( $P$ )	125.7	150.0

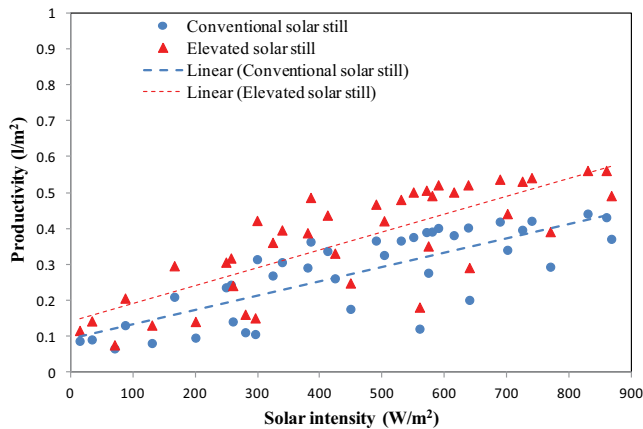


Fig. 11. Variations of the productivity as a function of solar intensity for two solar stills.

reveals that the daily average output for CSS and EBSS is 3.94 and 4.98 L/d. The stills are designed to last 10 y. The rate for CSS per litre is \$0.030, compared with around \$0.027 for the EBSS. These values show that, although the EBSS costs are higher, the output rise is higher. Therefore, total water costs decrease.

## 7. Conclusions

The main findings from this study are as follows:

- The daily fresh water yield of a CSS can be enhanced by lifting the basin of solar still.
- The EBSS shows higher fresh water productivity than the CSS, due to decrease in the heat loss from the bottom and side walls of solar still.
- The accumulated productivity values of the CSS are 3.02, 3.17, 3.39 and 3.63 L/m<sup>2</sup> for the months of February, March, April, and May, respectively. While, the productivity values of the EBSS are 4.14, 4.22, 4.42 and 4.73 L/m<sup>2</sup> for the same months.

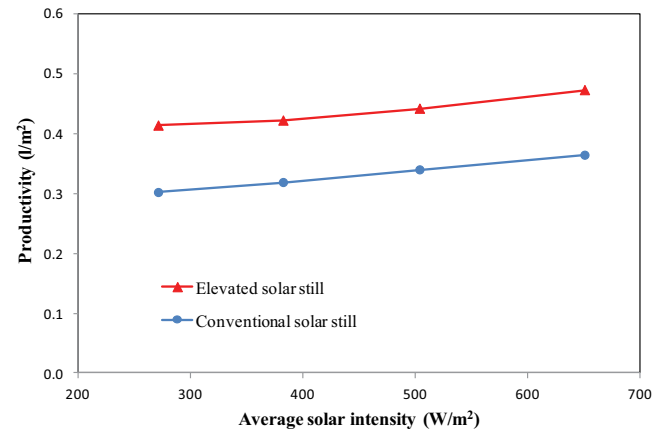


Fig. 12. Variations of the productivity as a function of average solar intensity for two solar stills.

- The improvement in the performance of the EBSS is inferred to be in between 37.0% and 47.0% over CSS.
- Simple cost analysis shows that the unit cost for distilled water for the CSS is \$30/m<sup>3</sup> while the unit cost for EBSS is lower and found to be approximately \$28.6/m<sup>3</sup>.

## Symbols

$A$	—	Area, m <sup>2</sup>
$\dot{m}$	—	Water production, kg/s
AMC	—	Annual maintenance and operating costs, \$
ASV	—	Annual salvage value, \$
$C_p$	—	Specific heat, J/kg K
CPL	—	Cost of fresh water, \$/L
CRF	—	Capital recovery factor
CSS	—	Conventional solar still
EBSS	—	Elevated basin solar still
$D$	—	Thermal diffusivity, m <sup>2</sup> /s
FAC	—	Fixed annual cost, \$
$g$	—	Gravity, m/s <sup>2</sup>
$h$	—	Coefficient of heat transfer, J/kg K
$H$	—	Trays height 0.5 cm
$h_{fg}$	—	Vaporization latent heat, J/kg
$i$	—	Interest rate, %
$I(t)$	—	Solar irradiation, W/m <sup>2</sup>
$K$	—	Thermal conductivity, W/m K
$L$	—	Length, m
$m$	—	Mass, kg
$M$	—	Average annual yield, L/y
$n$	—	Life time, years
$P$	—	Capital cost of solar still, \$
$P(t)$	—	Saturated vapor pressure, N/m <sup>2</sup>
$P_g$	—	Partial vapor pressure at glass temperature, N/m <sup>2</sup>
$P_w$	—	Partial vapor pressure at water temperature, N/m <sup>2</sup>
$Q$	—	Heat transfer rate, J
Ra	—	Rayleigh number
$S$	—	Salvage value
$t$	—	Time, s
$T$	—	Temperature, °C

TAC	—	Total annual cost, \$
$U$	—	Heat transfer coefficient, $W/m^2 K$
$V$	—	Wind speed, m/s
$W_R$	—	Uncertainty in the result

### Greek

$\alpha$	—	Absorptivity
$\beta$	—	Coefficient of thermal expansion
$\epsilon$	—	Emissivity
$\mu$	—	Dynamic viscosity, Pa.s
$\rho$	—	Density, $kg/m^3$
$\sigma$	—	Stefan–Boltzmann constant
$\delta$	—	Characteristic length, m
$\tau$	—	Transmissivity
$\eta_d$	—	Daily efficiency, %

### Subscripts

$a$	—	Ambient
$b$	—	Base
$c$	—	Convective
$e$	—	Evaporative
eff	—	Effective
fw	—	Feed water
$g$	—	Glass
$o$	—	Overall
$r$	—	Radiative
$s$	—	Side
$w$	—	Water
wb	—	Base water

### References

- [1] K. Sampathkumar, T.V. Arjunan, P. Pitchandi, P. Senthilkumar, Active solar distillation—a detailed review, *Renewable Sustainable Energy Rev.*, 14 (2010) 1503–1526.
- [2] A.A. Badran, A.A. Al-Hallaq, I.A. Salman, M.Z. Odat, A solar still augmented with a flat plate collector, *Desalination*, 172 (2005) 227–234.
- [3] H. Tanaka, Y. Nakatake, Effect of inclination of external flat plate reflector of basin type still in winter, *Sol. Energy*, 81 (2007) 1035–1042.
- [4] T. Rajaseenivasan, R. Nelson, K. Srithar, An experimental investigation on a solar still with an integrated flat plate collector, *Desalination*, 347 (2014) 131–137.
- [5] M.T. Chaichan, H.A. Kazem, Water solar distiller productivity enhancement using concentrating solar water heater and phase change material (PCM), *Case Stud. Therm. Eng.*, 5 (2015) 151–159.
- [6] H. Tanaka, Y. Nakatake, M. Tanaka, Indoor experiments of the vertical multiple-effect diffusion-type solar still coupled with a heat-pipe solar collector, *Desalination*, 177 (2005) 291–302.
- [7] V. Velmurugan, K. Srithar, Prospects and scopes of solar pond: a detailed review, *Renewable Sustainable Energy Rev.*, 12 (2008) 2253–2263.
- [8] W.H. Alawee, Improving the productivity of single effect double slope solar still by simple modification, *J. Eng.*, 21 (2015) 50–60.
- [9] W.H. Alawee, H.A. Dhahad, T.A. Mohamed, An Experimental Study on Improving the Performance of a Double Slope Solar Still, The 7th International Conference on Sustainable Agriculture for Food, Energy and Industry in Regional and Global Context, ICSAFEI-192, 2015.
- [10] H. Tanaka, Y. Nakatake, Increase in distillate productivity by inclining the flat plate external reflector of a tilted-wick solar still in winter, *Sol. Energy*, 83 (2009) 785–789.
- [11] A.S. Abdullah, M.M. Younes, Z.M. Omara, F.A. Essa, New design of trays solar still with enhanced evaporation methods—comprehensive study, *Sol. Energy*, 203 (2020) 164–174.
- [12] H. Tanaka, Experimental study of a basin type solar still with internal and external reflectors in winter, *Desalination*, 249 (2009) 130–134.
- [13] Z.M. Omara, Mofreh H. Hamed, A.E. Kabeel, Performance of finned and corrugate absorber solar stills under Egyptian conditions, *Desalination*, 277 (2011) 281–287.
- [14] R.P. Ayuthaya, P. Namprakai, W. Ampun, The thermal performance of an ethanol solar still with fin plate to increase productivity, *Renewable Energy*, 54 (2013) 227–234.
- [15] M.K. Kalidasa, K. Srithar, Performance study on basin type double slope solar still with different wick materials and minimum mass of water, *Renewable Energy*, 36 (2011) 612–620.
- [16] M. Sakthivel, S. Shanmugasundaram, T. Alwarsamy, An experimental study on a regenerative solar still with energy storage medium – jute cloth, *Desalination*, 264 (2010) 24–31.
- [17] T. Arunkumar, Effect of nano-coated CuO absorbers with PVA sponges in solar water desalting system, *Appl. Therm. Eng.*, 148 (2019) 1416–1424.
- [18] B. Panitapu, V. Koneru, L.S. Sagi Sri, A. Parik, Solar distillation using nano-material, *Int. J. Sci. Eng. Technol.*, 3 (2014) 583–587.
- [19] T. Elango, A. Kannan, M. Kalidasa, Performance study on single basin single slope solar still with different water nanofluids, *Desalination*, 360 (2015) 45–51.
- [20] M.T. Chaichan, H.A. Kazem, Single slope solar distillator productivity improvement using phase change material and  $Al_2O_3$  nanoparticle, *Sol. Energy*, 164 (2018) 370–381.
- [21] A. Somwanshi, A. Tiwari, Performance enhancement of a single basin solar still with flow of water from an air cooler on the cover, *Desalination*, 352 (2014) 92–102.
- [22] A.Z. Al-Garni, Productivity enhancement of solar still using water heater and cooling fan, *J. Solar Energy Eng.*, 134 (2012) 031006.
- [23] P.U. Suneesh, R. Jayaprakash, T.A. Kumar, D. Denkenberger, Effect of air flow on V type solar still with cotton gauze cooling, *Desalination*, 337 (2014) 1–5.
- [24] K. Kumar, R. Kasturibai, Performance study on solar still with enhanced condensation, *Desalination*, 230 (2008) 51–61.
- [25] Y.A. El-Samadony, A.S. Abdullah, Z.M. Omara, Experimental study of stepped solar still integrated with reflectors and external condenser, *Exp. Heat Transf.*, 28 (2015) 392–404.
- [26] A.E. Kabeel, Z.M. Omara, F.A. Essa, Enhancement of modified solar still integrated with external condenser using nanofluids: an experimental approach, *Energy Convers. Manage.*, 78 (2014) 493–498.
- [27] L. Zuo, Y. Zheng, Z. Li, Y. Sha, Experimental Investigation on the Effect of Cover Material on the Performance of Solar Still, International Conference on Sustainable Power Generation and Supply (SUPERGEN 2012), Hangzhou, doi: 10.1049/cp.2012.1774.
- [28] H. Aybar, H. Assefi, Simulation of a solar still to investigate water depth and glass angle, *Desal. Water Treat.*, 7 (2009) 35–40.
- [29] R. Dev, G.N. Tiwari, Characteristic equation of a passive solar still, *Desalination*, 245 (2009) 246–265.
- [30] F.A. Essa, Z.M. Omara, A.S. Abdullah, S. Shanmugan, H. Panchal, A.E. Kabeel, R. Sathyamurthy, W.H. Alawee, A. Muthu Manokar, A.H. Elsheikh, Wall-suspended trays inside stepped distiller with  $Al_2O_3$ /paraffin wax mixture and vapor suction: experimental implementation, *Energy Storage*, 32 (2020) 102008.
- [31] S. Abdallah, O.O. Badran, Sun tracking system for productivity enhancement of solar still, *Desalination*, 220 (2008) 669–676.
- [32] A.S. Abdullah, Z.M. Omara, M.A. Bek, F.A. Essa, An augmented productivity of solar distillers integrated to HDH unit: experimental implementation, *Appl. Therm. Eng.*, 167 (2020) 114723.
- [33] F.A. Essa, A.S. Abdullah, Z.M. Omara, A.E. Kabeel, W.M. El-Maghlany, On the different packing materials of humidification–dehumidification thermal desalination techniques—a review, *J. Cleaner Prod.*, 277 (2020) 123468.

- [34] A.E. Kabeel, Mofreh H. Hamed, Z.M. Omara, Augmentation of the basin type solar still using photovoltaic powered turbulence system, *Desal. Water Treat.*, 48 (2012) 182–190.
- [35] T. Arunkumar, K. Vinothkumar, A. Ahsan, R.1. Jayaprakash, S. Kumar, Experimental study on various solar still designs, *ISRN Renewable Energy*, (2012) 569381, doi: 10.5402/2012/569381.
- [36] Z.M. Omara, A.E. Kabeel, A.S. Abdullah, F.A. Essa, Experimental investigation of corrugated absorber solar still with wick and reflectors, *Desalination*, 381 (2016) 111–116.
- [37] P. Refalo, R. Ghirlando, S. Abela, The use of a solar chimney and condensers to enhance the productivity of a solar still, *Desal. Water Treat.*, 57 (2015) 23024–23037.
- [38] A.S. Abdullah, A. Alarjani, M.M. Abou Al-Sood, Z.M. Omara, A.E. Kabeel, F.A. Essa, Rotating-wick solar still with mended evaporation technics: experimental approach, *Alex. Eng. J.*, 58 (2019) 1449–1459.
- [39] F.A. Essa, A.S. Abdullah, Z.M. Omara, Rotating discs solar still: New mechanism of desalination, *J. Cleaner Prod.*, 275 (2020) 123200.
- [40] A.S. Abdullah, F.A. Essa, Z.M. Omara, Y. Rashid, L. Hadj-Taieb, G.B. bdelaziz, A.E. Kabeel, Rotating-drum solar still with enhanced evaporation and condensation techniques: comprehensive study, *Energy Convers. Manage.*, 199 (2019) 1120–1124.
- [41] J. Holman, *Experimental Methods for Engineers*, 8th ed., McGraw-Hill Companies, New York, 2012, pp. 63–64.
- [42] K. Srithar, *Studies on Solar Augmented Evaporation Systems for Tannery Effluent (Soak liquor)*, PhD Thesis, Indian Institute of Technology, Madras, 2003.
- [43] M. Appadurai, V. Velmurugan, Performance analysis of fin type solar still integrated with fin type mini solar pond, *Sustainable Energy Technol. Assess.*, 9 (2015) 30–36.
- [44] T.B. Nguyen, The mathematical model of basin-type solar distillation systems. *Distillation-Modeling, Simulation and Optimization*. Vilmar Steffen, Intech Open, doi: 10.5772/intechopen, (2019) 83228.
- [45] S.K. Shukla, V.P. Sorayan, Thermal modeling of solar stills; an experimental validation, *Renewable Energy*, 30 (2005) 683–699.
- [46] A.E. Kabeel, A. Khalil, Z.M. Omara, M.M. Younes, Theoretical and experimental parametric study of modified stepped solar still, *Desalination*, 289 (2012) 12–20.
- [47] Y.H. Zurigat, M.K. Abu-Arabi, Modeling and performance analysis of a regenerative solar desalination unit, *Appl. Therm. Eng.*, 24 (2004) 1061–1072.
- [48] A.E. Kabeel, A.M. Hamed, S.A. El-Agouz, Cost analysis of different solar still configurations, *Energy*, 35 (2010) 2901–2908.
- [49] M.M. Naim, M.A. Abd ElKawi, Non-conventional solar stills with energy storage element, *Desalination*, 153 (2003) 71–80.
- [50] M.T. Chaichan, K.I. Abass, H.A. Kazem, Design and assessment of solar concentrator distilling system using phase change materials (PCM) suitable for deserter weathers, *Desal. Water Treat.*, 57 (2016) 4897–14907.
- [51] W.H. Alawee, H.A. Dhahad, K.I. Abass, Increase the yield of simple solar distillation using the water drip method, *Int. J. Comput. Appl. Sci.*, 6 (2019) 447–445.
- [52] H.E. Fath, M. El-Samanoudy, K. Fahmy, A. Hassabou, Thermal-economic analysis and comparison between pyramid shaped and single-slope solar still configurations, *Desalination*, 159 (2003) 69–79.
- [53] S. Kumar, G.N. Tiwari, Life cycle cost analysis of single slope hybrid (PV/T) active solar still, *Appl. Energy*, 86 (2009) 1995–2004.

## Appendix A

To measure the increase of the condensation area, the following formula of a triangle was used:

$$A_c = \left( \frac{W_c}{\cos 30} \right) \times L = 2 \times \frac{0.30}{0.866} \times 1.25 = 0.866 \text{ m}^2 \quad (\text{A1})$$

$$A_m = \left( \frac{W_m}{\cos 30} \right) \times L = 2 \times \frac{0.55}{0.866} \times 1.25 = 1.58 \text{ m}^2 \quad (\text{A2})$$

$$\text{Percentage of increase\%} = \frac{A_m - A_c}{A_c} \quad (\text{A3})$$

$$\begin{aligned} \text{Percentage of increase of condensation area\%} &= \frac{1.58 - 0.866}{0.866} \\ &\times 100 = 82.4\% \end{aligned} \quad (\text{A4})$$

where  $A_c$  and  $A_m$  are the condensation surface areas of the basins used in the CSS and the EBSS, respectively.

## Appendix B

The unit cost of the distilled water ( $UC_{dw}$ ) can be computed using the formula from Kabeel et al. [48].

$$UC_{dw} = \frac{TAC}{M_{\text{yearly}}} \quad (\text{B1})$$

In the above,  $M_{\text{yearly}}$  is the average annual yield in L/m<sup>2</sup>, and TAC is the total annualised cost, and is determined as follows:

$$\begin{aligned} \text{Total annualised cost (TAC)} &= \text{First annual cost (FAC)} + \\ &\text{annual maintenance cost (AMC)} - \\ &\text{annual salvage value (ASV)} \end{aligned} \quad (\text{B2})$$

The FAC of a solar still is given as follows:

$$FAC = P \times (\text{CRF}) \quad (\text{B3})$$

The capital recovery factor (CRF) is determined as follows:

$$CRF = \frac{i(1+i)^n}{(1+i)^n - 1} \quad (\text{B4})$$

Here,  $n$  is the number of life years and  $i$  is the interest per year; these values are assumed as 10 y and 12%, respectively.

The AMC is assumed to be 15% of the fixed annual cost; hence, it is determined as follows:

$$AMC = 0.15(\text{FAC}) \quad (\text{B5})$$

ASV can be expressed as follows:

$$ASV = S \times (\text{SFF}) \quad (\text{B6})$$

The salvage value ( $S$ ) is assumed to be 10% of the annualised capital cost ( $P$ ) of the solar still, and the sinking fund factor is calculated as follows:

$$(\text{SFF}) = \frac{i}{(1+i)^n - 1} \quad (\text{B7})$$

Parameters	Value
Mass of glass, $M_g$	10.0 kg for CSS 18.5 kg for EBSS
Specific heat of glass, $C_{p,g}$	800 J/kg K
Area of glass, $A_g$	0.86 m <sup>2</sup> for CSS 1.58 m <sup>2</sup> for EBSS
Absorptivity of glass, $\alpha_g$	0.0475
Emissivities of water, $\epsilon_w$	0.96
Emissivities of glass, $\epsilon_g$	0.88
Mass of water, $M_w$	15 kg
Specific heat of water, $C_{p,w}$	4,187 J/kg °C
Absorptivity of water, $\alpha_w$	0.05
Area of water, $A_w$	0.75 m <sup>2</sup>
Mass of basin, $M_b$	5.2 kg
Specific heat of basin, $C_{p,w}$	473 J/kg °C
Absorptivity of basin, $\alpha_w$	0.95
Area of the basin plate, $A_b$	0.75 m <sup>2</sup>